

# Primary energy reconstruction from the $S(500)$ observable recorded with the KASCADE-Grande detector array

G. Toma<sup>§</sup>, W.D. Apel<sup>\*</sup>, J.C. Arteaga<sup>†,xi</sup>, F. Badea<sup>\*</sup>, K. Bekk<sup>\*</sup>, M. Bertina<sup>‡</sup>, J. Blümer<sup>\*,†</sup>, H. Bozdog<sup>\*</sup>, I.M. Brancus<sup>§</sup>, M. Brüggemann<sup>¶</sup>, P. Buchholz<sup>¶</sup>, E. Cantoni<sup>‡,||</sup>, A. Chiavassa<sup>‡</sup>, F. Cossavella<sup>†</sup>, K. Daumiller<sup>\*</sup>, V. de Souza<sup>†,xii</sup>, F. Di Pierro<sup>‡</sup>, P. Doll<sup>\*</sup>, R. Engel<sup>\*</sup>, J. Engler<sup>\*</sup>, M. Finger<sup>\*</sup>, D. Fuhrmann<sup>\*\*</sup>, P.L. Ghia<sup>||</sup>, H.J. Gils<sup>\*</sup>, R. Glasstetter<sup>\*\*</sup>, C. Grupen<sup>¶</sup>, A. Haungs<sup>\*</sup>, D. Heck<sup>\*</sup>, J.R. Hörandel<sup>†,xiii</sup>, T. Huege<sup>\*</sup>, P.G. Isar<sup>\*</sup>, K.-H. Kampert<sup>\*\*</sup>, D. Kang<sup>†</sup>, D. Kikelbick<sup>¶</sup>, H.O. Klages<sup>\*</sup>, P. Łuczak<sup>††</sup>, H.J. Mathes<sup>\*</sup>, H.J. Mayer<sup>\*</sup>, J. Milke<sup>\*</sup>, B. Mitrica<sup>§</sup>, C. Morello<sup>||</sup>, G. Navarra<sup>‡</sup>, S. Nehls<sup>\*</sup>, J. Oehlschläger<sup>\*</sup>, S. Ostapchenko<sup>\*,xiv</sup>, S. Over<sup>¶</sup>, M. Petcu<sup>§</sup>, T. Pierog<sup>\*</sup>, H. Rebel<sup>\*</sup>, M. Roth<sup>\*</sup>, H. Schieler<sup>\*</sup>, F. Schröder<sup>\*</sup>, O. Sima<sup>‡‡</sup>, M. Stümpert<sup>†</sup>, G.C. Trinchero<sup>||</sup>, H. Ulrich<sup>\*</sup>, A. Weindl<sup>\*</sup>, J. Wochele<sup>\*</sup>, M. Wommer<sup>\*</sup>, J. Zabierowski<sup>††</sup>

<sup>\*</sup>Institut für Kernphysik, Forschungszentrum Karlsruhe, 76021 Karlsruhe, Germany

<sup>†</sup>Institut für Experimentelle Kernphysik, Universität Karlsruhe, 76021 Karlsruhe, Germany

<sup>‡</sup>Dipartimento di Fisica Generale dell'Università, 10125 Torino, Italy

<sup>§</sup>National Institute of Physics and Nuclear Engineering, 7690 Bucharest, Romania

<sup>¶</sup>Fachbereich Physik, Universität Siegen, 57068 Siegen, Germany

<sup>||</sup>Istituto di Fisica dello Spazio Interplanetario, INAF, 10133 Torino, Italy

<sup>\*\*</sup>Fachbereich Physik, Universität Wuppertal, 42097 Wuppertal, Germany

<sup>††</sup>Soltan Institute for Nuclear Studies, 90950 Lodz, Poland

<sup>‡‡</sup>Department of Physics, University of Bucharest, 76900 Bucharest, Romania

<sup>xi</sup>now at: Universidad Michoacana, Morelia, Mexico

<sup>xii</sup>now at: Universidade de São Paulo, Instituto de Física de São Carlos, Brasil

<sup>xiii</sup>now at: Dept. of Astrophysics, Radboud University Nijmegen, The Netherlands

<sup>xiv</sup>now at: University of Trondheim, Norway

**Abstract.** Previous EAS investigations have shown that the charged particle density becomes independent of the primary mass at large but fixed distances from the shower core and that it can be used as an estimator for the primary energy. The particular radial distance from the shower axis where this effect takes place is dependent on the detector layout. For the KASCADE-Grande experiment it was shown to be around 500 m. A notation  $S(500)$  is used for the charged particle density at this specific distance. Extensive simulation studies have shown that  $S(500)$  is mapping the primary energy. We present results on the reconstruction of the primary energy spectrum of cosmic rays from the experimentally recorded  $S(500)$  observable using the KASCADE-Grande array. The constant intensity cut (CIC) method is applied to evaluate the attenuation of the  $S(500)$  observable with the zenith angle. A correction is subsequently applied to correct all recorded  $S(500)$  values for attenuation. The all event  $S(500)$  spectrum is obtained. A calibration of  $S(500)$  values with the primary energy has been worked out by simulations and has been used for conversion thus providing the possibility to obtain the primary energy spectrum (in the energy range accessible to the KASCADE-Grande array,  $10^{16}$ - $10^{18}$  eV). An evaluation of systematic uncertainties induced by different factors is also given.

**Keywords:** KASCADE-Grande, EAS, primary energy spectrum

## I. INTRODUCTION

Hillas has shown that the EAS particle density distributions at a certain distance from the shower core (dependent on the EAS detection array) becomes independent of the primary mass and can be used as a primary energy estimator [1]. Following this feature, a method can be derived to reconstruct the primary energy spectrum from the particular value of the charged particle density, observed at such specific radial ranges. The technique has been used by different detector arrays in order to reconstruct the primary energy spectrum of the cosmic radiation [2]. In the case of the KASCADE-Grande array (at Forschungszentrum Karlsruhe, Germany, 110 m a.s.l.) [3], detailed simulations [4] have shown that the particular distance for which this effect takes place is about 500 m (see fig. 1). Therefore an observable of interest in the case of KASCADE-Grande is the charged particle density at 500 m distance from the shower core, noted as  $S(500)$  in the following. The study has been performed for both simulated (fig. 1) and experimental (fig. 2) events, using identical reconstruction procedures [5]. The reconstruction begins with recording the energy deposits of particles in the KASCADE-Grande detector stations and the associated temporal information (arrival times of particles). The

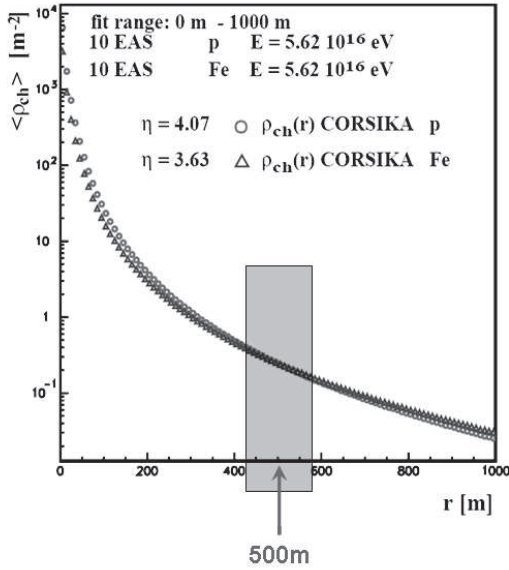


Fig. 1: Simulations show that, for the case of the KASCADE-Grande experimental layout, the particle density becomes independent of the primary mass around 500 m distance from shower core; this plot shows averaged simulated lateral distributions for different primary types with equal energy.

arrival direction of the shower is reconstructed from the particle arrival times. Using appropriate **Lateral Energy Correction Functions (LECF)**, the energy deposits are converted into particle densities. The LECF functions are dependent on the shower zenith angle [6] and take into account the fact that an inclined particle will deposit more energy in detectors due to its longer cross path. For every event, the obtained lateral density distribution is approximated by a Linsley [7] **Lateral Density Function (LDF)** in order to evaluate the particle density at the radial range of interest, 500 m. To ensure good reconstruction quality, the approximation is performed over a limited range of the lateral extension, namely only in the 40 m – 1000 m radial range.

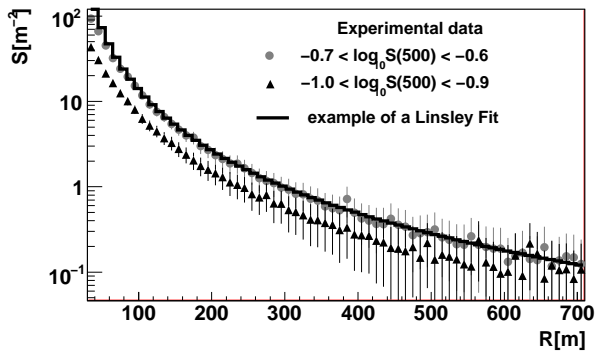


Fig. 2: Averaged lateral density distributions of experimentally recorded EAS samples for two  $S(500)$  ranges.

## II. EFFICIENCY AND QUALITY CUTS

For the experimental EAS sample, the total time of acquisition was  $\approx 902$  days. Showers were detected on a  $500 \times 600 \text{ m}^2$  area up to  $30^\circ$  zenith angle. The  $30^\circ$  zenith angle limit was imposed due to certain systematic effects affecting the reconstruction of small showers above this threshold. In order to ensure good reconstruction quality, several quality cuts were imposed on the data. The same cuts were used for both simulated and experimental events. Only those events are accepted for which the reconstructed shower core is positioned inside the detector array and not too close to the border. A good quality of the fit to the Linsley distribution is a further important criterion. Fig. 3 shows the total reconstruction efficiency for different zenith angle intervals (the full efficiency is reached at around  $\log_{10}(E_0/\text{GeV})=7.5$ ).

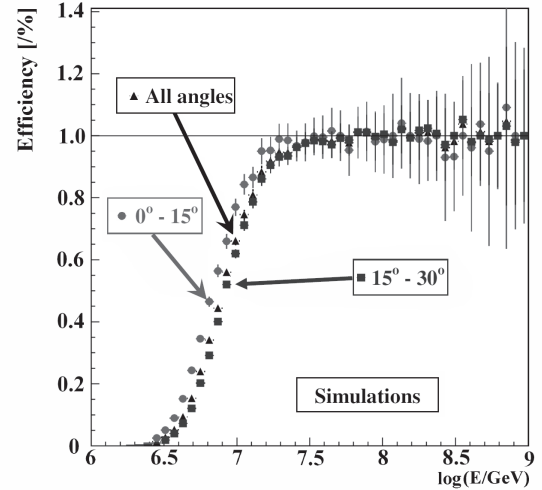


Fig. 3: Reconstruction efficiency for different zenith angle ranges and for the entire shower sample (events triggering more than 24 stations).

## III. THE CONSTANT INTENSITY CUT METHOD

Before converting the recorded  $S(500)$  values into the corresponding primary energy values (via a relation derived from simulation studies), one has to take into account the atmospheric attenuation affecting the charged particle densities observed on ground. For more inclined showers, the particles have to cross a longer path through the atmosphere before reaching the detector level. In such a case, events generated by identical primaries reach the detector level at different stages of EAS development, dependent on their angles of incidence. In order to bring all recorded EAS events to the same level of consistency, one has to eliminate the influence of the zenith angle on the recorded  $S(500)$  observables. This is achieved by applying the **Constant Intensity Cut (CIC)** method. The  $S(500)$  attenuation is visible if  $S(500)$  spectra are plotted for different EAS incident angles. For this, the recorded events are separated into several

sub-samples characterized by their angle of incidence. The angular intervals are chosen in a way that they open equal solid angles:  $0^\circ - 13.2^\circ$ ,  $13.2^\circ - 18.8^\circ$ ,  $18.8^\circ - 23.1^\circ$ ,  $23.1^\circ - 26.7^\circ$  and  $26.7^\circ - 30.0^\circ$ . In fig. 4 the attenuation is visible, as  $S(500)$  spectra are shifted towards lower values for increasing zenith angles. The CIC method assumes that a given intensity value in the energy spectrum corresponds to a given primary energy of particles and, since the  $S(500)$  is mapping the primary energy spectrum, it is expected that this property of the intensity is true also in the case of  $S(500)$  spectra. Therefore a constant intensity cut on integral  $S(500)$  spectra is performed, effectively cutting them at a given primary energy. The intersection of the cut line with each spectrum will give the attenuated  $S(500)$  value at the corresponding angle of incidence for a given primary energy. A linear interpolation is used between the two neighboring points in the integral spectrum in order to convert the value of the intensity into particle density for each angular bin. The observed attenuation can be corrected by parameterizing the attenuation curve and correcting all events by bringing their  $S(500)$  value to their corresponding value at a given reference angle of incidence (see fig. 5; the parameterization with the lowest  $\chi^2$  was chosen, namely the one corresponding to intensity 3000). For the present study this angle is considered to be  $21^\circ$ , since the zenith angular distribution for the recorded EAS sample peaks at this value. The CIC method implies several mathematical transformations of data before obtaining the values corrected for attenuation of the  $S(500)$  observable: interpolations and analytical parameterizations (as mentioned in the above description of the CIC method). These operations introduce some systematic uncertainties on the final result of the CIC method. The CIC-induced systematic uncertainty of the corrected  $S(500)$  value is evaluated by propagating the errors of fit parameters. The resulting CIC-induced error of the  $S(500)$  observable will be taken into account later when evaluating the total systematic uncertainty of the reconstructed primary energy.

#### IV. CONVERSION TO ENERGY

After correcting the recorded  $S(500)$  values for attenuation, we can proceed to convert each of them to the corresponding primary energy value. A calibration of the primary energy  $E_0$  with  $S(500)$  was derived from simulations (see fig. 6). The Monte-Carlo CORSIKA EAS simulation tool was used to simulate air showers (with QGSJET II model embedded for high energy interactions). In fig. 6, two slightly different dependencies are shown for two primaries, a light primary (proton) and a heavy primary (Fe). The two dependencies are almost identical, a feature that is expected due to the mass insensitivity of the  $S(500)$  observable. This calibration is used to convert all  $S(500)$  values into the corresponding primary energies. The spectrum of primary energy is thus reconstructed. Fig. 7 shows the reconstructed energy spectrum compared with spectra reconstructed by

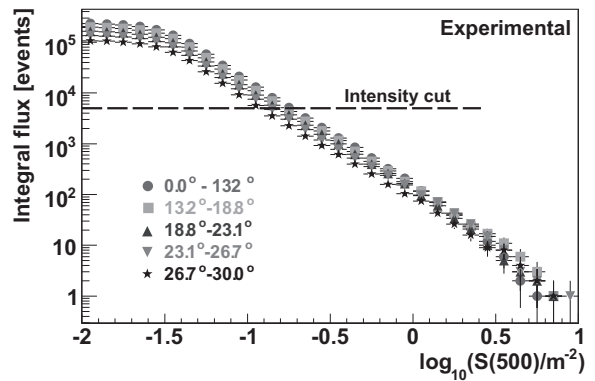


Fig. 4: Integral  $S(500)$  spectra; the horizontal line is a constant intensity cut at an arbitrarily chosen intensity; attenuation length of  $S(500)$  was evaluated at  $347.38 \pm 21.65 \text{ g} \cdot \text{cm}^{-2}$

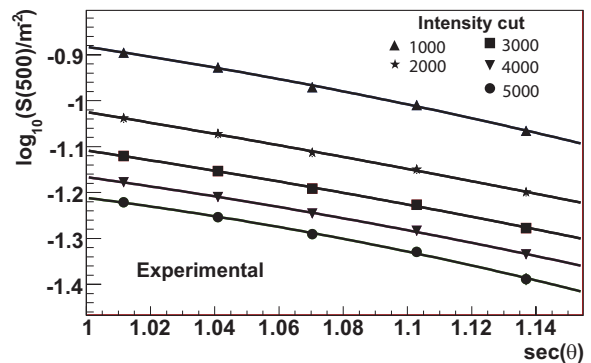


Fig. 5: Attenuation of the  $S(500)$  observable with the angle of incidence; the different curves show different arbitrarily chosen intensity cuts.

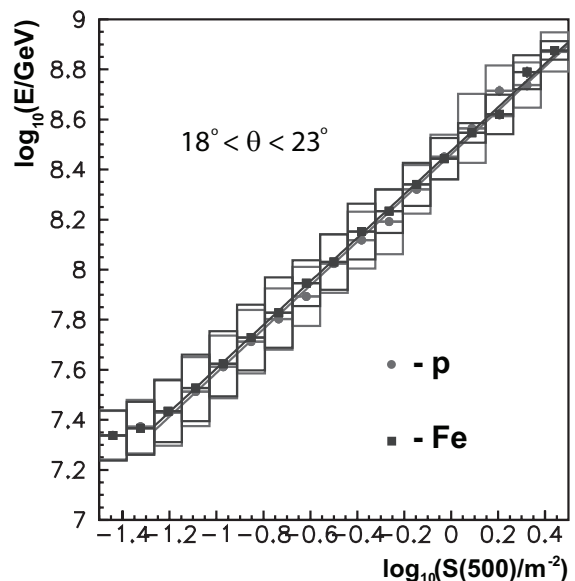


Fig. 6:  $E_0 - S(500)$  calibration curve for two different primaries; the box-errors are the errors on the spread; the errors on the mean are represented with bars.

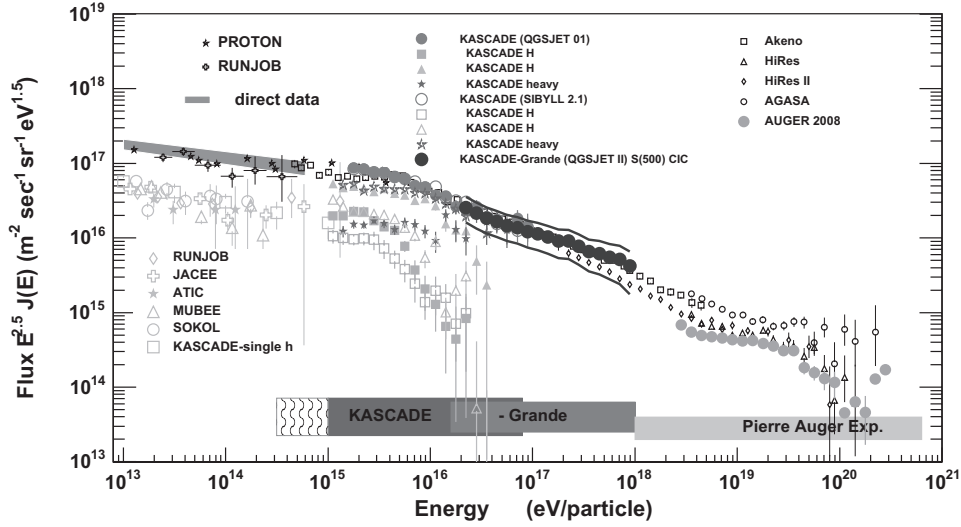


Fig. 7: Reconstructed experimental energy spectrum by KASCADE-Grande from  $S(500)/CIC$ , multiplied by  $E^{2.5}$  compared with results of other experiments; the continuous lines above and below the spectrum are the error envelopes and show combined statistical and systematic uncertainties.

other experiments. The spectrum is plotted starting from the maximum efficiency threshold (see fig. 3). For the systematic contribution to the total error, several sources of systematic uncertainties have been identified and their contributions were evaluated. Thus, the spectral index of the simulated shower sample was equal to  $-2$  and was acting as a source of systematic uncertainty. In a similar fashion, the  $S(500)-E_0$  calibration and the CIC method itself were also introducing systematic uncertainties. In all, these three sources were contributing with an uncertainty of  $\approx 1\%$  from the total flux value. Other sources that were considered were the Monte-Carlo statistical uncertainty of the simulated shower sample and the choosing of a certain reference angle at which to perform the  $S(500)$  attenuation correction (contributing with  $\approx 7\%$  and  $\approx 30\%$  relative uncertainty). The relative contribution of all identified sources over the full efficiency range was fairly constant for any given source and in total amounts for about 37% of the recorded flux value. The energy resolution has also been evaluated from simulations by calculating the difference between the true and the reconstructed primary energy (applying CIC to the simulated data). The energy resolution was found to be 22% for  $E_0=10^{17}$  eV (for all primaries) and is fairly constant over the entire full efficiency range.

## V. CONCLUSIONS

The primary energy spectrum has been reconstructed from the particle densities recorded in the stations of the KASCADE-Grande array. In the particular case of KASCADE-Grande, the charged particle density at 500 m distance from the shower core was shown to be primary mass insensitive. The CIC method was applied on the recorded  $S(500)$  spectrum in order to correct

each shower for attenuation effects. Using a simulation-derived calibration between  $S(500)$  and  $E_0$  (based on the QGSJET II model for high energy interactions), the attenuation corrected  $S(500)$  spectrum has been converted into primary energy spectrum. The  $S(500)$  derived KASCADE-Grande spectrum is composition independent and comes in good agreement with the spectrum of lower energies previously reconstructed by the KASCADE array. Future investigations will concentrate also on improving the quality of the reconstruction along with gaining a better understanding of the uncertainties induced by the reconstruction technique.

## ACKNOWLEDGMENT

The KASCADE-Grande experiment is supported by the BMBF of Germany, the MIUR and INAF of Italy, the the Polish Ministry of Science and Higher Education (grant 2009-2011), and the Romanian Ministry of Education and Research.

## REFERENCES

- [1] A.M. Hillas et al., Proc.12th ICRC, Hobart 3 (1971) 1001
- [2] D.M. Edge et al., J. Phys. A: Math. Nucl. Gen.6 (1973) 1612; M. Nagano et al., J. Phys. G:Nucl. Part. Phys.10(1984) 1295; Y. Dai et al., J.Phys.G: Nucl. Part. Phys. 14(1998) 793; M. Roth et al.- Auger collaboration Proc. 28th ICRC, Tsukuba, Japan, vol. 2 (2003) 333
- [3] A. Haungs et al., KASCADE-Grande collaboration, Proc. 28th ICRC, Tsukuba, Japan, vol.2 (2003)985
- [4] H. Rebel and O. Sima et al. KASCADE-Grande collaboration, Proc. 29th ICRC, Pune, India, vol.6 (2005)297 I.M. Brancus et al. KASCADE-Grande collaboration, Proc. 29th ICRC, Pune, India, vol.6 (2005)361
- [5] O. Sima et al., Report FZKA 6985, Forschungszentrum Karlsruhe 2004
- [6] G. Toma et al., Proc. 26th ECRS 2006, Lisbon, Portugal, so-134; CERN program library, GEANT users guide, (1997)
- [7] J. Linsley et al., Journ. Phys. Soc. Japan 17 (1962) A-III